

An Iron-Porphyrin Complex with Large Easy-Axis Magnetic Anisotropy on Metal Substrate

Bing Liu,^{†,‡} Huixia Fu,^{†,‡} Jiaqi Guan,^{†,‡} Bin Shao,[§] Sheng Meng,^{*,†,‡,||} Jiandong Guo,^{*,†,‡,||} and Weihua Wang^{*,†}

[†]Beijing National Laboratory for Condensed Matter Physics and Institute of Physics, Chinese Academy of Sciences, Beijing 100190, China

[‡]School of Physical Sciences, University of Chinese Academy of Sciences, Beijing 100190, China

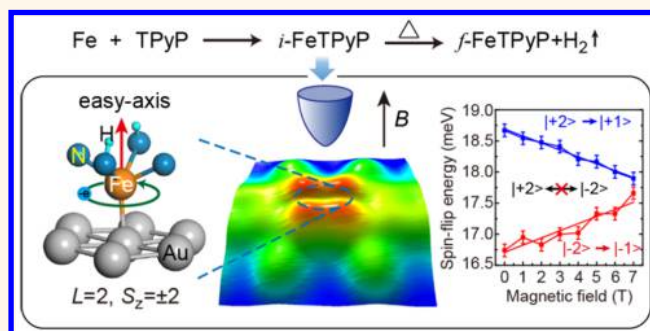
[§]Bremen Center for Computational Materials Science, University of Bremen, 28359 Bremen, Germany

^{||}Collaborative Innovation Center of Quantum Matter, Beijing 100871, China

Supporting Information

ABSTRACT: Easy-axis magnetic anisotropy separates two magnetic states with opposite magnetic moments, and single magnetic atoms and molecules with large easy-axis magnetic anisotropy are highly desired for future applications in high-density data storage and quantum computation. By tuning the metalation reaction between tetra-pyridyl-porphyrin molecules and Fe atoms, we have stabilized the so-called initial complex, an intermediate state of the reaction, on Au(111) substrate, and investigated the magnetic property of this complex at a single-molecule level by low-temperature scanning tunneling microscopy and spectroscopy. As revealed by inelastic electron tunneling spectroscopy in magnetic field, this Fe-porphyrin complex has magnetic anisotropy energy of more than 15 meV with its easy-axis perpendicular to the molecular plane. Two magnetic states with opposite spin directions are discriminated by the dependence of spin-flip excitation energy on magnetic field and are found to have long spin lifetimes. Our density functional theory calculations reveal that the Fe atom in this complex, decoupled from Au substrate by a weak ligand field with elongated Fe–N bonds, has a high-spin state $S = 2$ and a large orbital angular momentum $L = 2$, which give rise to easy-axis anisotropy perpendicular to the molecular plane and large magnetic anisotropy energy by spin-orbit coupling. Since the Fe atom is protected by the molecular ligand, the complex can be processed at room or even higher temperatures. The reported system may have potential applications in nonvolatile data storage, and our work demonstrates on-surface metalation reactions can be utilized to synthesize organometallic complexes with large magnetic anisotropy.

KEYWORDS: magnetic anisotropy, spin lifetime, on-surface reaction, scanning tunneling microscopy, inelastic electron tunneling spectroscopy, spin-flip excitation, organometallic complex



Magnetic anisotropy describes the directionality and stability of spontaneous magnetization. In magnetic systems with easy-axis magnetic anisotropy, two magnetic states with opposite magnetic moments are separated by an energy barrier and may have long magnetic relaxation times.^{1,2} For the ultimate goal to realize high-density data storage and quantum computation using single atoms or molecules,^{3–5} there is an ongoing pursuit of single magnetic atoms and molecules with large easy-axis magnetic anisotropy.^{6–8} For most magnetic atoms adsorbed on metal substrates, their magnetic moments are easily screened or even quenched by itinerant electrons,^{9,10} while only rare cases show magnetic anisotropy energy of no more than 10 meV on Pt(111) surface.^{11–13} To achieve large magnetic anisotropy, an insulating layer was used to decouple the magnetic atoms

from metal substrates, whereas this strategy requires the system to be prepared and kept at low temperature.^{7,14–16} In organometallic complexes, the molecular ligands provide an alternative way to decouple magnetic atoms from metal substrates.^{17,18} Moreover, the ligand field surrounding the magnetic atom can determine its spin and orbital degrees of freedom and thus dictates its magnetic anisotropy by spin-orbit coupling.^{19,20} In this scenario, a ligand field that can keep the magnetic atom in high-spin state and preserve its orbital angular momentum is highly desired.²¹ Until now, although various

Received: August 24, 2017

Accepted: October 24, 2017

Published: October 24, 2017

surface-adsorbed organometallic complexes were reported to show magnetic anisotropy energy in the order of several millielectronvolts,^{22–26} organometallic complexes with easy-axis magnetic anisotropy have been rarely addressed.^{22,25} It still remains a challenge to realize large easy-axis magnetic anisotropy in organometallic complexes.

During the on-surface metalation reaction between free-base porphyrin molecules and metal atoms, the metal atom is lifted from substrate to the molecular plane.²⁷ Although metalloporphyrins containing Fe or Co atoms show a Kondo effect,^{28,29} different magnetic properties can be expected in the intermediate state of the metalation reaction, or the so-called “initial complex”,²⁷ with magnetic atoms. In this initial complex, the metal atom is coordinated to the nonhydrogenated porphyrin macrocycle, but not fully incorporated into it.^{30–32} Thus, the ligand field surrounding the metal atom in the initial complex is much weaker than that in the final product, which may affect the spin and orbital angular momentum of the metal atom. However, until now such initial complexes with magnetic atoms (such as Fe, Co, and Ni) have never been observed experimentally.²⁷

Scanning tunneling microscopy and spectroscopy (STM/STS) are powerful tools to identify the reactants, intermediates, and products of on-surface reactions^{32,33} and to investigate the magnetic properties of single atoms and molecules.^{6,14,15,34} The magnetic anisotropy energy of a single atom or molecule is measured as the zero-field splitting (ZFS) energy in inelastic electron tunneling spectroscopy (IETS), which is the spin-flip excitation energy in the absence of external magnetic field.^{7,14,15,22}

In this work, by tuning the metalation reaction between tetrapyrrolyl-porphyrin (TPyP, see Figure 1a) molecules and Fe atoms on Au(111) substrate, we have stabilized the initial complex of this reaction in a metastable state and investigated this complex by STM/STS at a single-molecule level. IETS in magnetic field indicates that this organometallic complex has magnetic anisotropy energy of more than 15 meV with easy-axis perpendicular to the molecular plane. Two magnetic states with opposite spin directions are discriminated by IETS in varied magnetic fields and are found to have long spin lifetimes. Our density functional theory (DFT) calculations reveal that the Fe atom in this complex, surrounded by a delicate ligand field with elongated Fe–N bonds and weak coordination to substrate Au atoms, has a high-spin state $S = 2$ and a large orbital angular momentum $L = 2$, which give rise to easy-axis magnetic anisotropy perpendicular to the molecular plane and large magnetic anisotropy energy by spin-orbit coupling.

RESULTS AND DISCUSSION

After Fe and TPyP molecules are deposited sequentially onto a Au(111) substrate, one-dimensional (1D) chains and two-dimensional (2D) islands are formed. These structures are similar to previously reported TPyP-Fe self-assemblies on Au(111), in which TPyP molecules are linked side by side through pyridyl–Fe–pyridyl coordination bonds.^{18,35} A careful investigation shows that there are three types of molecules on the surface (see Supporting Information Figure S1). Figure 1b shows a section of chain containing all three types of molecules, and the three molecules from bottom to top are denoted as type-I, type-II and type-III. All of these molecules show intramolecular patterns with C_{2v} symmetry: type-I shows a depression in the center, type-II shows a depressed center and four bright lobes separated by two bisecting lines along the

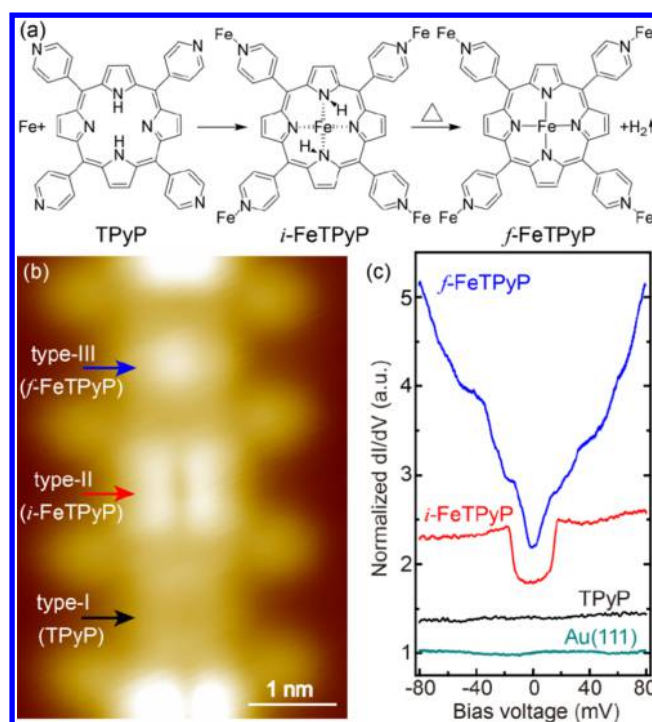


Figure 1. (a) On-surface metalation reaction between TPyP molecules and Fe atoms. (b) STM image (−1.5 V, 100 pA) of type-I (TPyP), type-II (*i*-FeTPyP) and type-III (*f*-FeTPyP) molecules. (c) Representative dI/dV spectra of the three types of molecules and bare Au(111) surface near the Fermi level. The spectra were measured with tip stabilized at 80 mV and 400 pA for type-I (TPyP), 80 mV and 300 pA for type-II (*i*-FeTPyP), and 80 mV and 600 pA for type-III (*f*-FeTPyP) and bare Au(111). These spectra were normalized by being divided by the values near Fermi level and then vertically shifted by 0.4.

molecular high-symmetry axes, and type-III shows a rod-like protrusion sandwiched between two shoulder features along one high-symmetry axis.

Since type-I molecules are similar to the TPyP molecules in the absence of Fe (Supporting Information Figure S2), they are attributed to free-base TPyP molecules. Type-III molecules show close resemblance to previously reported Fe(II)-porphyrin molecules synthesized through on-surface metalation reactions,^{29,36,37} thus we ascribe type-III to *f*-FeTPyP, the final product of the metalation reaction (see Figure 1a). Based on STM experiments (Supporting Information Section 2), type-II is identified as the initial complex of the metalation reaction between Fe and TPyP (Figure 1a) and denoted as *i*-FeTPyP to be distinguished from the final product *f*-FeTPyP.

The representative dI/dV spectra measured near the Fermi level at the centers of the three types of molecules are compared in Figure 1c, together with a spectrum of bare Au(111) surface for reference. The dI/dV spectrum measured on TPyP molecule and Au(111) are featureless in the range of −80 meV to +80 meV. In contrast, *i*-FeTPyP shows two symmetric conductance steps at ±15 meV, while *f*-FeTPyP shows multiple conductance steps.

These dI/dV spectra of *i*-FeTPyP and *f*-FeTPyP are interpreted as IETS, and the differential conductance steps are attributed to opening of additional inelastic electron tunneling channels when the energy of tunneling electrons exceeds certain thresholds. The IETS measured on *i*-FeTPyP indicates an excitation process with excitation energy of 15

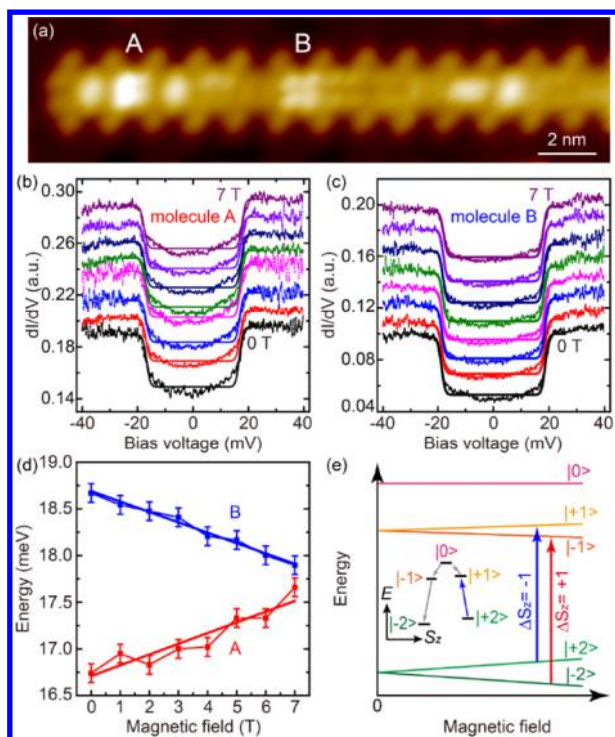


Figure 2. (a) STM image of a molecular chain containing two *i*-FeTPyP molecules, denoted as A and B (−1.5 V, 50 pA). (b and c) dI/dV spectra measured at the centers of molecule A and B with the same tip in perpendicular magnetic field from 0 to 7 T at an interval of 1 T. The spectra are vertically shifted for clarity. The tip was stabilized at $V = 40$ mV and $I = 500$ pA when measuring the spectra. The fitting lines of respective spectra are plotted in solid lines of the same color. (d) Excitation energies extracted from the fitting lines in (b) and (c). The error bars are given by the amplitude of sinusoidal modulation. The red and blue lines are the fittings of the spin-flip excitation energy in molecule A and B, respectively. (e) Schematic of the energy levels of $S = 2$ states in magnetic field. The spin-flip excitation energy increases with magnetic field for the $\Delta S_z = +1$ excitation (indicated by red arrow), while decreases for the $\Delta S_z = -1$ excitation (indicated by blue arrow). Inset: The multiple spin-flip transitions from $|+2\rangle$ to $|−2\rangle$ state, with threshold energy defined by the blue arrow.

meV. To unveil the origin of this excitation, we measured IETS on *i*-FeTPyP in magnetic fields perpendicular to the substrate (Figure 2). For each IETS, the excitation energy is derived by fitting the spectrum with two temperature-broadened step functions distributed symmetrically with respect to the Fermi level:

$$\sigma(eV) = \sigma_0 + h^- \theta(\varepsilon + eV) + h^+ \theta(\varepsilon - eV) \quad (1)$$

where $\sigma(eV)$ is the measured differential conductance at bias V , ε is the electron charge, σ_0 describes the nonzero background, h^- (h^+) is the height of inelastic step at negative (positive) bias polarity, ε is the excitation energy and

$$\theta(\varepsilon) = \frac{1 + (x - 1) \exp(x)}{(\exp(x) - 1)^2} \quad (2)$$

with $x = \varepsilon/k_B T$, k_B is the Boltzmann's constant, and T is the temperature.³⁸

Figure 2a shows two *i*-FeTPyP molecules, denoted as A and B, in the same chain. The least-squares fits of IETS measured on the two molecules are plotted in Figure 2b,c, respectively

(Supporting Information Section 3). Figure 2d shows the dependence of the extracted excitation energies on magnetic field. The excitation energy varies with magnetic field, which is a signature of Zeeman splitting, and indicates the observed excitation is caused by the spin-flip process.^{14,15,39} The excitation energy of molecule A increases from 16.7 ± 0.1 meV at 0 T to 17.7 ± 0.1 meV at 7 T, while the excitation energy of molecule B decreases from 18.7 ± 0.1 meV at 0 T to 17.9 ± 0.1 meV at 7 T. As discussed below, the inverse trends are given by different spin-flip ground states that have opposite spin directions.

To the lowest order, the spin excitation of the Fe atom in *i*-FeTPyP molecule is modeled by a spin Hamiltonian:^{15,22,38}

$$\hat{H} = g\mu_B \vec{B} \cdot \hat{S} + D\hat{S}_z^2 + E(\hat{S}_x^2 - \hat{S}_y^2) \quad (3)$$

The first term represents the Zeeman splitting caused by external magnetic field, in which g is the Landé factor, μ_B is the Bohr magneton, and $\hat{S} = (\hat{S}_x, \hat{S}_y, \hat{S}_z)$ is the spin operator. The second (third) term describes the axial (transverse) magnetic anisotropy, with D (E) the axial (transverse) magnetic anisotropy parameter.

Our DFT calculations indicate the Fe atom in *i*-FeTPyP molecule has a spin state of $S = 2$ (discussed below), which is also in agreement with previous result of similar Fe-porphyrin system.²⁹ Diagonalization of eq 3 with $S_z = |+2\rangle, |+1\rangle, |0\rangle, |-1\rangle$, and $|-2\rangle$ yields the eigenstates and eigenenergies. By fitting the measured excitation energies to spin-flip excitation energies, we found that the primary anisotropy axis, that is, the z axis in eq 3, is assigned to the direction perpendicular to the molecular plane (parallel to the magnetic field),⁴⁰ and the best fit gives $D = -5.57 \pm 0.01$ meV, $E = 0.00 \pm 0.01$ meV, and $g = 1.98 \pm 0.01$ for molecule A and $D = -6.23 \pm 0.01$ meV, $E = 0.00 \pm 0.01$ meV, and $g = 1.92 \pm 0.01$ for B.

The negative axial magnetic anisotropy parameter D means this system has an easy-axis magnetic anisotropy along the z axis, that is, perpendicular to the molecular plane. The transverse anisotropy parameter E is close to zero for both A and B, which minimizes the intermixing of different spin states and makes \hat{H} commute with \hat{S}_z (with magnetic field along the z direction). In this situation, \hat{H} and \hat{S}_z share the same eigenstates (see Figure 2e). Based on the equation given by C. F. Hirjibehedin *et al.*,¹⁵ the relative IETS step heights for transitions in different magnetic fields should be identical, which can be seen in Supporting Information Figure S5.

The fitted excitation energies are plotted in Figure 2d and are in good agreement with experimental results. The excitations in A and B correspond to spin-flip excitations from $|−2\rangle$ to $|−1\rangle$ with $\Delta S_z = +1$ and $|+2\rangle$ to $|+1\rangle$ with $\Delta S_z = -1$, respectively. Thus, molecule A is at a spin-flip ground state of $|−2\rangle$ and molecule B at $|+2\rangle$, that is, they have opposite spin directions along z axis. Note that the exact ZFS energies of the two molecules are different, and Figure 2e shows the dependence of $\Delta S_z = +1$ and $\Delta S_z = -1$ spin-flip excitation energies on magnetic field. The spin orientation in different *i*-FeTPyP molecules can also be detected by a spin-polarized tip with out-of-plane sensitivity.^{6–8} However, in our experiment, such spin-polarized measurements are not possible. We discern the spin-flip ground states by the dependence of spin-flip energy on magnetic field, which gives not only the spin orientation but also the spin states.

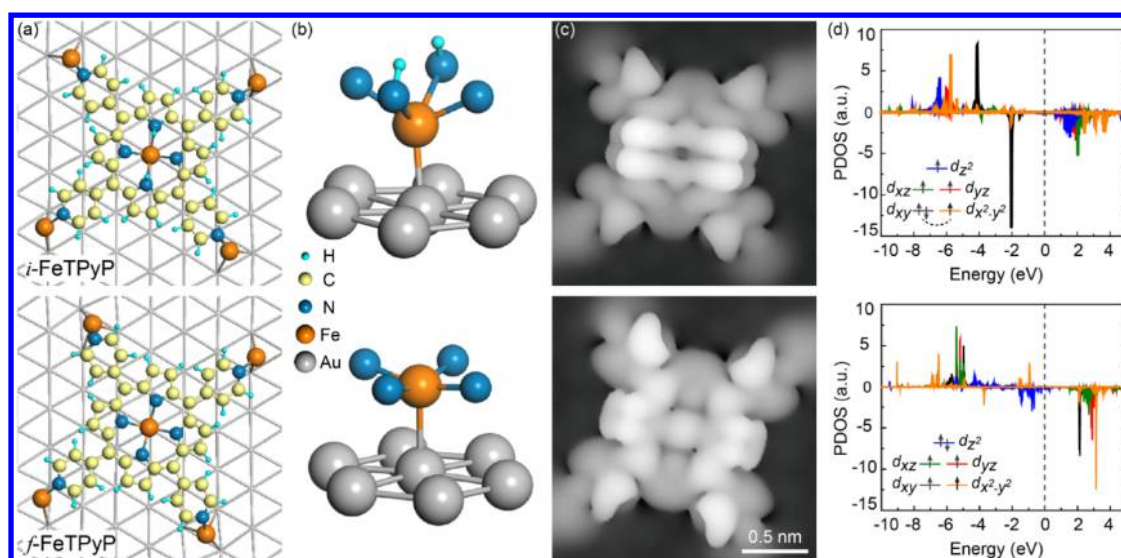


Figure 3. (a) Optimized adsorption configurations of (upper) *i*-FeTPyP and (lower) *f*-FeTPyP on Au(111), respectively. (b) The atoms surrounding Fe in (upper) *i*-FeTPyP and (lower) *f*-FeTPyP according to (a). (c) DFT simulated STM image of (upper) *i*-FeTPyP and (lower) *f*-FeTPyP at -1.0 V. (d) Calculated spin-polarized PDOS of the d-orbitals of the central Fe atom in (upper) *i*-FeTPyP and (lower) *f*-FeTPyP. The occupations of the d-orbitals are shown in the insets.

At zero field, the measured ZFS energy gives the energy difference between the ground state and an excited state, which has less spin projection on z axis. The measured ZFS energies indicate molecule A has a magnetic anisotropy energy of 16.7 meV, and molecule B has a magnetic anisotropy energy of 18.7 meV. It is worth noting that the measured ZFS energies are irrespective of junction impedance, but do vary from molecule to molecule (Supporting Information Section 3). For molecules with different values of ZFS energy, the spin-flip excitation energy either increases or decreases with magnetic field, as represented by molecule A and B, respectively. These results are in contrast to single Fe atoms on Au(111) surface, which are featureless around Fermi level at 6 K.¹⁰ The measured magnetic anisotropy energies in *i*-FeTPyP complexes are significantly larger than reported values for single atoms or molecules on metal substrates^{11–13,22–26} and exceed the magnetic anisotropy energy of single Fe atom on MgO.¹⁶

Considering the transverse anisotropy parameter $E = 0$ in the spin Hamiltonian, at zero magnetic field the $|+2\rangle$ and $|-2\rangle$ states are degenerate and separated by an energy barrier of $4|D|$ (>20 meV). The external magnetic field lifts the degeneracy between these two states and makes $|-2\rangle$ state energetically favorable. In this case, the $|+2\rangle$ state can switch to $|-2\rangle$ either by multiple spin-flip excitations (inset of Figure 2e) or magnetic tunnelling.^{1,6,8} Obviously, the thermal energy given by the environmental temperature of 4.9 K is insufficient to induce such multiple spin-flip excitations which have a threshold energy of 17.9 meV at 7 T (the spin excitation energy from $|+2\rangle$ to $|+1\rangle$ state). In our experiment, both the $|-2\rangle$ state in molecule A and the $|+2\rangle$ state in molecule B were stable in a magnetic field of 7 T for more than 15 h, indicating that in *i*-FeTPyP, the magnetic tunnelling between $|+2\rangle$ and $|-2\rangle$ states is suppressed, and the magnetic states $|+2\rangle$ and $|-2\rangle$ have long spin lifetimes. This long spin lifetime is a benefit from a transverse magnetic anisotropy parameter close to zero,¹ and the reported *i*-FeTPyP complexes may have potential applications in nonvolatile data storage.

The large easy-axis magnetic anisotropy of *i*-FeTPyP complex originates from the special ligand field surrounding

the central Fe atom. Figure 3a,b compares the optimized adsorption configurations of *i*-FeTPyP and *f*-FeTPyP. The simulated STM images reproduce well the topographical features observed in experiment (Figure 3c), further validating the proposed structure models of *i*-FeTPyP and *f*-FeTPyP. As illustrated in Figure 3b, the central Fe atom in *i*-FeTPyP does not sit in the same plane as the molecular backbone, but lies between the Au substrate and the molecular plane. The central Fe atom is 1.01 and 1.09 Å lower than iminic ($-\text{N}=\text{C}$) and pyrrolic ($-\text{NH}-$) nitrogen atoms, respectively. In *f*-FeTPyP, Fe is further lifted up from the Au substrate by 0.66 Å, being much closer to the molecular plane, which accounts for the changes of brightness at the molecular centers in their STM images. Consequently, the Fe–N bonds in *i*-FeTPyP, especially those with H attached (Fe–pyrrolic N ~ 2.43 Å, Fe–iminic N ~ 2.17 Å), are greatly elongated by more than 16% with respect to the Fe–N bonds in *f*-FeTPyP (~ 2.09 Å). As a result, the ligand field surround the Fe atom in *i*-FeTPyP is weaker than that in *f*-FeTPyP.

The calculated projected density of states (PDOS) of the d-orbitals of the central Fe atom in *i*-FeTPyP (Figure 3d) indicates only the d_{xy} orbital, partially overlapped with $d_{x^2-y^2}$ orbital, is doubly occupied, and the other orbitals are singly occupied by electrons with the same spin direction (inset of Figure 3d). Due to the relatively weak in-plane ligand field, the spin-orbit coupling together with the mixture of in-plane orbitals (d_{xy} and $d_{x^2-y^2}$) acts easily to restore an unquenched orbital angular momentum perpendicular to the molecular plane. Thus, the Fe atom in *i*-FeTPyP is in its 5D spin configuration ($L = 2$ and $S = 2$), which can give rise to a large magnetic anisotropy energy by spin-orbit coupling.⁷ Moreover, the dominant in-plane orbital motions can direct the electron spins parallel to the orbital angular momentum by spin-orbit coupling and results in easy-axis anisotropy perpendicular to the molecular plane.²² In contrast, the occupations of d-orbitals of the Fe atom in *f*-FeTPyP is drastically changed by its relatively strong in-plane bonds with N atoms. The doubly occupied orbital is not the mixture of d_{xy} and $d_{x^2-y^2}$ but d_{z^2} instead, that is, the Fe atom is in 5S term ($L = 0$). Therefore,

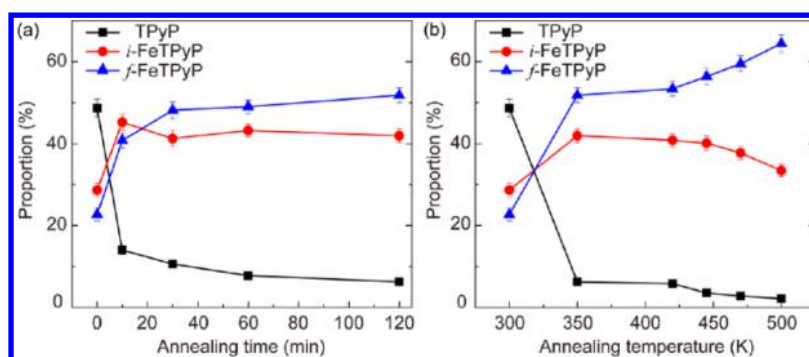


Figure 4. (a) Proportions of three types of molecules as a function of annealing time at 350 K. (b) Proportions of three types of molecules as a function of annealing temperature. The sample was annealed at each temperature for 30 min except at 350 K for 120 min. The error bars were given by $\sqrt{n_i}/N$, where n_i is the number of each type of molecules, and N up to 1500–2000 is the total number of molecules counted at each annealing stage.

the out-of-plane orbital motions are dominant in *f*-FeTPyP (Figure 3d).

The calculated spin-orbital configurations for Fe atom in *i*-FeTPyP and *f*-FeTPyP explain well the large easy-axis magnetic anisotropy in *i*-FeTPyP observed in experiment, which results from its local chemical environment contributed by both the hydrogen atoms on pyrrolic N atoms and the weak coupling to substrate Au atoms underneath.

In our experiments, the maximum proportion of *i*-FeTPyP complex was achieved to ~45% by moderate annealing at 350 K for 30 min, while the proportion of *i*-FeTPyP is hardly changed by extended annealing time at the same annealing temperature (Figure 4a). On the other hand, although higher annealing temperature promotes the reaction from *i*-FeTPyP to *f*-FeTPyP, some *i*-FeTPyP complexes still survive on the surface after annealed at 500 K.

It is worth to note that this *i*-FeTPyP intermediate has not been observed before.²⁷ Previous DFT calculations suggested the metalation reaction between porphyrin and Fe had no virtual barriers,³⁰ and other porphyrin derivatives were metalated smoothly by Fe atoms near room temperature. On Ag(111) substrate tetra-phenyl-porphyrin (TPP) and octaethylporphyrin (OEP) were metalated by postdeposited Fe atoms at room temperature,^{37,41} and TPyP were metalated at 320 K in the absence of pyridyl-Fe coordination.³⁶ In our comparative experiment between TPP and excess Fe on Au(111) substrate, all the TPP molecules were metalated into final product *f*-FeTPP at room temperature (Supporting Information Figure S8), in good agreement with the results on Ag(111).³⁷ The observation of *i*-FeTPyP in our experiment indicates this complex is in a metastable state in the reaction path, and the survival of *i*-FeTPyP after annealed to 500 K (Figure 4b) implies a considerable energy barrier is raised in the reaction path from *i*-FeTPyP to *f*-FeTPyP. By comparing the metalation reaction of TPyP in the presence of pyridyl-Fe coordination and the above metalation reactions, we believe the pyridyl-Fe coordination at peripheral groups may raise the reaction barrier from *i*-FeTPyP to *f*-FeTPyP, and more work is needed to reveal the detailed mechanism.

CONCLUSIONS

In conclusion, we have synthesized the initial complex of the on-surface metalation reaction between TPyP molecules and Fe atoms in a controlled way and achieved large easy-axis magnetic anisotropy in these complexes. The IETS in magnetic field

discriminated two magnetic states of opposite spin directions with long spin lifetimes. Since the Fe atom is protected by molecular ligand, the complex can be processed at room or even higher temperatures. We expect this method can be applied to other magnetic atoms and further combined with on-surface coordination or coupling reactions to fabricate nanostructures with multiple magnetic centers. The reported Fe-porphyrin complex may have potential applications in nonvolatile data storage, and our work demonstrates on-surface metalation reactions can be utilized to synthesize organo-metallic complexes with large magnetic anisotropy.

METHODS

All of the experiments were conducted in an ultrahigh-vacuum low-temperature scanning tunneling microscope (Unisoku) with a base pressure better than 1.0×10^{-10} Torr. The Au(111) substrate was cleaned by cycles of Ar⁺ sputtering and annealing. Excess Fe and submonolayer TPyP molecules were deposited on Au(111) substrate held at room temperature. The *dI/dV* spectra were acquired using a lock-in amplifier with a sinusoidal modulation of 987.5 Hz at 0.1 mV. The *I-t* spectra shown in Supporting Information were acquired by positioning the tip above the molecule, opening the feedback loop, switching the bias voltage to +2.8 V, and recording the tunneling current as a function of time. All of the experimental results were obtained at 4.9 K.

DFT calculations were performed using projector-augmented wave (PAW) pseudopotential and plane-wave basis set with energy cutoff at 400 eV. The van der Waals (vdW) density functional computations in conjunction with the Perdew–Burke–Ernzerhof (PBE) functional were performed to give accurate adsorption configurations. The calculation model was constructed by a Au(111)-(8 × 8) surface containing three Au atomic layers, in which the topmost layer was fully relaxed with the bottom two layers fixed. A vacuum region larger than 15 Å was applied. Structural optimizations adopted gamma-point-only K sampling, and all the structures were optimized until the force on each atom was <0.04 eV/Å. An effective Hubbard term $U = 4.0$ eV was added to describe the d-orbitals of the Fe atoms. All the calculations were performed with Vienna *Ab initio* Simulation Package (VASP).

ASSOCIATED CONTENT

Supporting Information

The Supporting Information is available free of charge on the ACS Publications website at DOI: 10.1021/acsnano.7b06029.

Additional STM results of three types of molecules on Au(111) substrate, revealing the structure of type-II molecule by STM, more details about IETS, and metalation reaction between Fe and TPP molecules on Au(111) surface (PDF)

AUTHOR INFORMATION

Corresponding Authors

*E-mail: smeng@iphy.ac.cn.

*E-mail: jdguo@iphy.ac.cn.

*E-mail: weihuawang@iphy.ac.cn.

ORCID

Sheng Meng: 0000-0002-1553-1432

Jiandong Guo: 0000-0002-7893-022X

Weihua Wang: 0000-0002-2269-1952

Notes

The authors declare no competing financial interest.

ACKNOWLEDGMENTS

We thank Prof. Yifeng Yang, Prof. Xingqiang Shi, Prof. Ziliang Shi, Dr. Tao Lin and Mr. Kai Li for useful discussions. This work is supported by the National Key Research and Development Program of China (grant nos. 2017YFA0303600 and 2016YFA0300600) and the Hundred Talents Program of the Chinese Academy of Sciences. S.M. is grateful to the financial support from Ministry of Science and Technology of China (grant nos. 2016YFA0300902 and 2015CB921001).

REFERENCES

- (1) Sangregorio, C.; Ohm, T.; Paulsen, C.; Sessoli, R.; Gatteschi, D. Quantum Tunneling of the Magnetization in an Iron Cluster Nanomagnet. *Phys. Rev. Lett.* **1997**, *78*, 4645–4648.
- (2) Freedman, D. E.; Harman, W. H.; Harris, T. D.; Long, G. J.; Chang, C. J.; Long, J. R. Slow Magnetic Relaxation in a High-Spin Iron(II) Complex. *J. Am. Chem. Soc.* **2010**, *132*, 1224–1225.
- (3) Leuenberger, M. N.; Loss, D. Quantum Computing in Molecular Magnets. *Nature* **2001**, *410*, 789–793.
- (4) Wolf, S. A.; Awschalom, D. D.; Buhrman, R. A.; Daughton, J. M.; von Molnár, S.; Roukes, M. L.; Chtchelkanova, A. Y.; Treger, D. M. Spintronics: A Spin-Based Electronics Vision for the Future. *Science* **2001**, *294*, 1488–1495.
- (5) Khajetoorians, A. A.; Heinrich, A. J. Toward Single-Atom Memory. *Science* **2016**, *352*, 296–297.
- (6) Loth, S.; Etzkorn, M.; Lutz, C. P.; Eigler, D. M.; Heinrich, A. J. Measurement of Fast Electron Spin Relaxation Times with Atomic Resolution. *Science* **2010**, *329*, 1628–1630.
- (7) Rau, I. G.; Baumann, S.; Rusponi, S.; Donati, F.; Stepanow, S.; Gragnaniello, L.; Dreiser, J.; Piamonteze, C.; Nolting, F.; Gangopadhyay, S.; Albertini, O. R.; Macfarlane, R. M.; Lutz, C. P.; Jones, B. A.; Gambardella, P.; Heinrich, A. J.; Brune, H. Reaching the Magnetic Anisotropy Limit of a 3d Metal Atom. *Science* **2014**, *344*, 988–992.
- (8) Paul, W.; Yang, K.; Baumann, S.; Romming, N.; Choi, T.; Lutz, C. P.; Heinrich, A. J. Control of the Millisecond Spin Lifetime of an Electrically Probed Atom. *Nat. Phys.* **2017**, *13*, 403–407.
- (9) Madhavan, V.; Chen, W.; Jamneala, T.; Crommie, M. F.; Wingreen, N. S. Tunneling into a Single Magnetic Atom: Spectroscopic Evidence of the Kondo Resonance. *Science* **1998**, *280*, 567–569.
- (10) Jamneala, T.; Madhavan, V.; Chen, W.; Crommie, M. F. Scanning Tunneling Spectroscopy of Transition-Metal Impurities at the Surface of Gold. *Phys. Rev. B: Condens. Matter Mater. Phys.* **2000**, *61*, 9990–9993.
- (11) Gambardella, P.; Rusponi, S.; Veronese, M.; Dhesi, S. S.; Grazioli, C.; Dallmeyer, A.; Cabria, L.; Zeller, R.; Dederichs, P. H.; Kern, K.; Carbone, C.; Brune, H. Giant Magnetic Anisotropy of Single Cobalt Atoms and Nanoparticles. *Science* **2003**, *300*, 1130–1133.
- (12) Khajetoorians, A. A.; Schlenk, T.; Schweflinghaus, B.; dos Santos Dias, M.; Steinbrecher, M.; Bouhassoune, M.; Lounis, S.; Wiebe, J.; Wiesendanger, R. Spin Excitations of Individual Fe Atoms on Pt(111): Impact of the Site-Dependent Giant Substrate Polarization. *Phys. Rev. Lett.* **2013**, *111*, 157204.
- (13) Miyamachi, T.; Schuh, T.; Märkl, T.; Bresch, C.; Balashov, T.; Stöhr, A.; Karlewski, C.; André, S.; Marthaler, M.; Hoffmann, M.; Geilhufe, M.; Ostanin, S.; Hergert, W.; Mertig, I.; Schön, G.; Ernst, A.; Wulfhchel, W. Stabilizing the Magnetic Moment of Single Holmium Atoms by Symmetry. *Nature* **2013**, *503*, 242–246.
- (14) Heinrich, A. J.; Gupta, J. A.; Lutz, C. P.; Eigler, D. M. Single-Atom Spin-Flip Spectroscopy. *Science* **2004**, *306*, 466–469.
- (15) Hirjibehedin, C. F.; Lin, C.-Y.; Otte, A. F.; Ternes, M.; Lutz, C. P.; Jones, B. A.; Heinrich, A. J. Large Magnetic Anisotropy of a Single Atomic Spin Embedded in a Surface Molecular Network. *Science* **2007**, *317*, 1199–1203.
- (16) Baumann, S.; Donati, F.; Stepanow, S.; Rusponi, S.; Paul, W.; Gangopadhyay, S.; Rau, I. G.; Pacchioni, G. E.; Gragnaniello, L.; Pivetta, M.; Dreiser, J.; Piamonteze, C.; Lutz, C. P.; Macfarlane, R. M.; Jones, B. A.; Gambardella, P.; Heinrich, A. J.; Brune, H. Origin of Perpendicular Magnetic Anisotropy and Large Orbital Moment in Fe Atoms on MgO. *Phys. Rev. Lett.* **2015**, *115*, 237202.
- (17) Gambardella, P.; Stepanow, S.; Dmitriev, A.; Honolka, J.; de Groot, F. M. F.; Lingenfelder, M.; Gupta, S. S.; Sarma, D. D.; Bencok, P.; Stanescu, S.; Clair, S.; Pons, S.; Lin, N.; Seitsonen, A. P.; Brune, H.; Barth, J. V.; Kern, K. Supramolecular Control of the Magnetic Anisotropy in Two-Dimensional High-Spin Fe Arrays at a Metal Interface. *Nat. Mater.* **2009**, *8*, 189–193.
- (18) Lin, T.; Kuang, G.; Wang, W.; Lin, N. Two-Dimensional Lattice of Out-of-Plane Dinuclear Iron Centers Exhibiting Kondo Resonance. *ACS Nano* **2014**, *8*, 8310–8316.
- (19) Carlin, R. L. Paramagnetism: Zero-Field Splittings. In *Magnetochemistry*; Springer-Verlag: Berlin, 1986; pp 19–34.
- (20) Getzlaff, M. Magnetic Anisotropy Effects. In *Fundamentals of Magnetism*; Springer-Verlag: Berlin, 2008; pp 89–115.
- (21) Yosida, K. Magnetic Ions in Crystals. In *Theory of Magnetism*; Springer-Verlag: Berlin, 1996; pp 25–48.
- (22) Tsukahara, N.; Noto, K.-i.; Ohara, M.; Shiraki, S.; Takagi, N.; Takata, Y.; Miyawaki, J.; Taguchi, M.; Chainani, A.; Shin, S.; Kawai, M. Adsorption-Induced Switching of Magnetic Anisotropy in a Single Iron(II) Phthalocyanine Molecule on an Oxidized Cu(110) Surface. *Phys. Rev. Lett.* **2009**, *102*, 167203.
- (23) Heinrich, B. W.; Braun, L.; Pascual, J. I.; Franke, K. J. Protection of Excited Spin States by a Superconducting Energy Gap. *Nat. Phys.* **2013**, *9*, 765–768.
- (24) Heinrich, B. W.; Braun, L.; Pascual, J. I.; Franke, K. J. Tuning the Magnetic Anisotropy of Single Molecules. *Nano Lett.* **2015**, *15*, 4024–4028.
- (25) Stoll, P.; Bernien, M.; Rolf, D.; Nickel, F.; Xu, Q.; Hartmann, C.; Umbach, T. R.; Kopprasch, J.; Ladenthin, J. N.; Schierle, E.; Weschke, E.; Czekelius, C.; Kuch, W.; Franke, K. J. Magnetic Anisotropy in Surface-Supported Single-Ion Lanthanide Complexes. *Phys. Rev. B: Condens. Matter Mater. Phys.* **2016**, *94*, 224426.
- (26) Ormaza, M.; Bachellier, N.; Faraggi, M. N.; Verlhac, B.; Abufager, P.; Ohresser, P.; Joly, L.; Romeo, M.; Scheurer, F.; Bocquet, M.-L.; Lorente, N.; Limot, L. Efficient Spin-Flip Excitation of a Nickelocene Molecule. *Nano Lett.* **2017**, *17*, 1877–1882.
- (27) Gottfried, J. M. Surface Chemistry of Porphyrins and Phthalocyanines. *Surf. Sci. Rep.* **2015**, *70*, 259–379.
- (28) Iancu, V.; Deshpande, A.; Hla, S.-W. Manipulating Kondo Temperature via Single Molecule Switching. *Nano Lett.* **2006**, *6*, 820–823.
- (29) Wang, W.; Pang, R.; Kuang, G.; Shi, X.; Shang, X.; Liu, P. N.; Lin, N. Intramolecularly Resolved Kondo Resonance of High-Spin Fe(II)-Porphyrin Adsorbed on Au(111). *Phys. Rev. B: Condens. Matter Mater. Phys.* **2015**, *91*, 045440.
- (30) Shubina, T. E.; Marbach, H.; Flechtner, K.; Kretschmann, A.; Jux, N.; Buchner, F.; Steinrück, H.-P.; Clark, T.; Gottfried, J. M. Principle and Mechanism of Direct Porphyrin Metalation: Joint Experimental and Theoretical Investigation. *J. Am. Chem. Soc.* **2007**, *129*, 9476–9483.

(31) Doyle, C. M.; Krasnikov, S. A.; Sergeeva, N. N.; Preobrajenski, A. B.; Vinogradov, N. A.; Sergeeva, Y. N.; Senge, M. O.; Cafolla, A. A. Evidence for the Formation of an Intermediate Complex in the Direct Metalation of Tetra(4-bromophenyl)-Porphyrin on the Cu(111) Surface. *Chem. Commun.* **2011**, *47*, 12134–12136.

(32) Li, Y.; Xiao, J.; Shubina, T. E.; Chen, M.; Shi, Z.; Schmid, M.; Steinrück, H.-P.; Gottfried, J. M.; Lin, N. Coordination and Metalation Bifunctionality of Cu with 5,10,15,20-Tetra(4-pyridyl)porphyrin: Toward a Mixed-Valence Two-Dimensional Coordination Network. *J. Am. Chem. Soc.* **2012**, *134*, 6401–6408.

(33) Wang, W.; Shi, X.; Wang, S.; Hove, M. V.; Lin, N. Single-Molecule Resolution of an Organometallic Intermediate in a Surface-Supported Ullmann Coupling Reaction. *J. Am. Chem. Soc.* **2011**, *133*, 13264–13267.

(34) Zhao, A.; Li, Q.; Chen, L.; Xiang, H.; Wang, W.; Pan, S.; Wang, B.; Xiao, X.; Yang, J.; Hou, J. G.; Zhu, Q. Controlling the Kondo Effect of an Adsorbed Magnetic Ion Through Its Chemical Bonding. *Science* **2005**, *309*, 1542–1544.

(35) Wang, Y.; Zhou, K.; Shi, Z.; Ma, Y.-q. Structural Reconstruction and Spontaneous Formation of Fe Polynuclears: a Self-Assembly of Fe–Porphyrin Coordination Chains on Au(111) Revealed by Scanning Tunneling Microscopy. *Phys. Chem. Chem. Phys.* **2016**, *18*, 14273–14278.

(36) Auwärter, W.; Weber-Bargioni, A.; Brink, S.; Riemann, A.; Schiffrin, A.; Ruben, M.; Barth, J. V. Controlled Metalation of Self-Assembled Porphyrin Nanoarrays in Two Dimensions. *ChemPhysChem* **2007**, *8*, 250–254.

(37) Buchner, F.; Schwald, V.; Comanici, K.; Steinrück, H.-P.; Marbach, H. Microscopic Evidence of the Metalation of a Free-Base Porphyrin Monolayer with Iron. *ChemPhysChem* **2007**, *8*, 241–243.

(38) von Bergmann, K.; Ternes, M.; Loth, S.; Lutz, C. P.; Heinrich, A. J. Spin Polarization of the Split Kondo State. *Phys. Rev. Lett.* **2015**, *114*, 076601.

(39) Ternes, M. Spin Excitations and Correlations in Scanning Tunneling Spectroscopy. *New J. Phys.* **2015**, *17*, 063016.

(40) We tried the cases of B//x and B//y, but the fittings showed large discrepancy from the experimental results.

(41) Borghetti, P.; Santo, G. D.; Castellarin-Cudia, C.; Fanetti, M.; Sangaletti, L.; Magnano, E.; Bondino, F.; Goldoni, A. Adsorption Geometry, Conformation, and Electronic Structure of 2H-Octaethylporphyrin on Ag(111) and Fe Metalation in Ultra High Vacuum. *J. Chem. Phys.* **2013**, *138*, 144702.